行政院國家科學委員會專題研究計畫 成果報告

含胜肽分子之氫氧基磷灰石/鈦功能性漸鍍層之特性研究 (第 2 年)
研究成果報告(完整版)

計 畫 類 別 ：個別型
計 畫 編 號 ：NSC 95-2314-B-040-011-MY2
執 行 期 間 ：96 年 08 月 01 日至 97 年 07 月 31 日
執 行 單 位 ：中山醫學大學口腔材料科學研究所

計 畫 主 持 人：丁信智
共 同 主 持 人：陳震漢
計畫參與人員：碩士班研究生-兼任助理人員：何佳哲
碩士班研究生-兼任助理人員：王偉仲

報 告 附 件 ：出席國際會議研究心得報告及發表論文

處 理 方 式 ：本計畫涉及專利或其他智慧財產權，2 年後可公開查詢

中 華 民 國 97 年 09 月 02 日

目錄

1. 中文摘要

具生物活性的氫氧基磷灰石鍍層已經使用在需承載負荷的植體應用上。本貳年計劃著重利用電漿披覆技術披覆功能性 HA/Ti 複合漸層，此漸層由上層 HA 活性層，中間交互層 HA/Ti 及下層 Ti 鍵結層構成，以改善鍍層-基材間介面性質，此後並將 HA/Ti 複合漸層熱處理以便接枝 RGD 胜肽。目前第一年之結果指出 HA/Ti 漸層之表面化學及微結構類似純 HA 鍍層，但鍵結強度較優。HA 鍍層經循環疲勞後強度顯著下降 23%，而 HA/Ti 漸層無多大影響。電化學測試也顯示 HA/Ti 複合漸層性質優於純 HA 鍍層。第二年主要是利用 400–700^{o}C 熱處理提高鍍層結晶性，評估抗腐蝕能力及鍵結強度。Gentamicin 釋放及 RGD 接枝亦是另一重點。結果發現適當熱處理可以提高鍍層結晶性及提高抗腐蝕能力，與更有效釋放 gentamicin 抗生素。RGD 接枝方面經 MTT 分析則顯示細胞貼附能力並未受到 RGD 或熱處理所影響。鍍層在 600^{o}C 熱處理可提高其結晶性與減少缺陷，並不影響強度等優點，也許是一提升 HA/Ti 漸層性能之適當處理方式。

關鍵詞：鈦、氫氧基磷灰石、漸層、植體、電漿披覆、胜肽

2. 英文摘要

Bioceramic coatings like hydroxyapatite (HA) have shown promising bioactive properties in load-bearing implant applications. The two-year project is to deposit functionally graded HA/Ti layers consisting of an underlying Ti bond coat, the alternating layer, and an HA top-layer on Ti6Al4V substrates using plasma spray to improve the coating-substrate interface properties. The alternating layers were created by means of changing the feeding rate and input power of Ti and HA powders, which gradually decreasing Ti content with increasing depth from the Ti bond-coat. After which, characterization of RGD peptide-grafted coatings following heat treatment will be emphasized. The presently first-year results indicated that surface chemistry and morphology of the graded coatings were similar to those of monolithic HA coatings. The bond strength values of the as-sprayed graded coatings were much superior to those of monolithic HA coatings. The cyclic fatigue did have a statistically significant effect on bond strength of monolithic HA coatings, with a decrease of 23%. However, the graded coatings were able to survive 1 million cycles of loading in air without significantly reduced bond strength. The *in vitro* electrochemical measurement results also indicated that the graded coatings had a more beneficial and desired behavior than monolithic HA coatings after fatigue. In the secondary year, the major consideration was to examine the corrosion resistance and bond strength of graded coatings after various postheat treatment temperatures ranging from 400^{o}C to 700^{o}C. Gentamicin loading onto the plasma-sprayed coating was used to improve its antibacterial activity. RGD grafting is also another focus. Our results indicate that an appropriate heat treatment resulted in recrystallization of amorphous calcium phosphate of the as-sprayed coatings. The enhancement in corrosion resistance took place after heat treatment. Gentamicin loading might provide effective release at early time points (up to 1 h). As for RGD grafting on coating surface, the MTT assay indicated there are no significant differences between all samples with or without RGDC peptide. The heat treatment at 600^{o}C for 1 h in air, leading to increased crystallinity and fewer defects, as well as enhanced bond strength, may be a suitable post-deposition treatment method to promote the characteristics of graded HA/Ti coatings that also serve as a drug carrier.

Keywords: Titanium, hydroxyapatite, graded coating, implant, plasma spray, peptide

3. 緣由與目的

HA-coated implants have shown promising bioactive properties in orthorpaedic and dental surgery [1-2]. A variety of coating techniques, such as plasma spraying [1], magnetron sputtering [3], and sol-gel processing [4], have been explored to coat HA onto metals. Among these techniques, plasma spraying is perhaps most popularly used due to its process feasibility such as ease of operation. However, the plasma-sprayed HA coatings generally contained cracks, pores, second phases, and residual stresses that can reduce their durability and lead to partial or complete delamination of the coatings in body fluids [5]. In addition, the major causes of failure of HA-coated implants appear to reside in the coating-substrate interface [6,7]. In a study by Kangasniemi et al. [7] the failure mode of bone-HA interfacial tensile testing was observed to occur consistently at the HA-Ti interface, indicating clearly that it was difficult to develop reliable HA/Ti alloy bonding.

The adhesion of the HA coating to its Ti substrate and the integrity of the substrate/coating interface are always concerned in determining the performance and reliability of any HA-coated devices. Short-term clinical trials have shown HA coatings to enhance bone apposition, fixation, and reduce healing time. Nevertheless, the long-term stability of such coatings was the predominate factor causing the success of the implant. For improving the coating-substrate bond strength and other properties, many attempts have been made to develop biocoatings with higher strength. In this case, double layer or multiplayer coatings have been considered recently [6,8]. The deposition of a composite coating, wherein a metallic phase is introduced to serve as either an intermediate layer (bond coat) or a second (continuous or dispersed) phase in the HA matrix was pursued to enhance the interface properties. For example, Gu et al. [6] used a approach of ceramic slurry mixing to prepare composite powders with an inner core of Ti6Al4V particles swathed by a layer of mixed HA/ yttria stabilized zirconia powders for plasma spraying onto Ti6Al4V substrates.

Another more effective approach in the design of eliminating material-property discontinuities to significantly increase adhesion strength is by means of grading the material composition near the interfaces or through the coatings, so-called functionally graded materials. The top layer of functionally graded coatings may provide good bioactive properties to accelerate bone healing and the underlying bond coat may be designed to achieve maximum adhesion strength. Between these two layers is a transition layer with intermediate properties. Gruner developed a multi-layered coating composed of a Ti precoat, a Ti/HA composite layer and an HA top-layer by plasma deposition [9]. This implant study showed a fast and stable fusion between the coated implant and the bone. Inagaki et al. [10] plasma-sprayed gradient-like HA/Ti composite coatings at different RF power and suggested that the bond strength increased with increasing power of plasma due to the increase in density of the coatings. However, their work did not provide the results of cyclic fatigue and corrosion behaviors of the potent graded coatings, which are of paramount importance, when implanted in body [9,10].

It is believed that HA coatings with higher crystallinity always yield a decreased dissolution rate [11] and enhanced rate of cell proliferation [12]. In order to improve the quality of plasma-sprayed coatings further than optimizing plasma spray processing and altering material composition [13], heat treatment is sometimes used to increase coating crystallinity and reduce the residual stress of HA-based coatings [14–16]. In a recent paper [17], we found that treatment at 600^{o}C could play a predominant role in enhancing the characteristics of plasma-sprayed HA coatings.

Bacterial infection of bone is still a non-negligible concern in dental and orthopedic surgery. In the treatment of carious teeth, bacteria left in the cavity of infected dentin are one of the factors leading to secondary caries or pulpal injury after restoration [18]. Antibacterial

treatment of the cavity is thus recommended before restoration is completed. Systems of controlled release can target delivery of biologically active agents to specific bone tissue areas for enhanced healing and repair. Local delivery can yield higher concentrations in the relevant tissues, improving their efficacy and possibly reducing the necessary duration of treatment [19].

Extracellular matrix (ECM) proteins contain signaling domains which can be synthesized as bioactive peptide fragments. Many biomaterials have been modified with short peptides in an effort to enhance cell-material interactions, and mimic the role of ECM proteins [20,21]. The best studied of these peptides is the RGD sequence, a motif that binds to integrin cell adhesion receptors and thereby promotes cell attachment to the material surface. The use of RGD-peptide may be a future way of improving biomaterial surface. According to the literature [22,23], the autologous human bone marrow stroma cells may be successfully associated to RGD-grafted biomaterials Ti to promote cell colonization.

In the present project, the graded coatings were plasma-sprayed onto Ti6Al4V substrates. By independently changing the feeding rate and plasma power of the Ti and HA powders, compositional control of the coating was achieved. It was attempted to combine the advantages of both the high chemical affinity between the underlying coating containing Ti and Ti6Al4V substrate and functionally graded coating concepts. The focus was to investigate the cyclic fatigue resistance of plasma-sprayed coatings using three-point bending test. The coating morphology, crystal structure and bond strength were also characterized. Next, to further enhance the quality of the potential HA/Ti graded coatings by means of post-deposition heat treatment was achieved. Additionally, combining osteoconductive properties of bioactive coatings with an antibiotic release could produce a two-fold beneficial effect. Finally, the evaluation of RGD grafting on coatings was another focus.

4. 實驗方法

4.1. Fabrication of graded coatings

Commercial HA powder (AMDRY 6021, Plasma Technik A.G., Wohlen, Switzerland) with particle size between 44 and 149 μm was used in this study. Pure Ti particles of 100 μm were purchased from Alloy Metals Inc (AMDRY 918, Troy, MI). Commercially available plates of Ti6Al4V alloy (100 × 10 × 3 thick) were used as the substrate material. Prior to plasma spray, the substrate surface was mechanically polished to #1200 grit level, cleaned and sandblasted with 450 μm SiC particles. To obtain a uniform coating, the substrate was mounted on a disk that could rotate during spraying in air using a Plasma-Technik A-3000 system (Plasma Technik A.G., Wohlen, Switzerland).

Functionally graded HA/Ti coatings consisting of an underlying Ti bond coat, the alternating layer, and an HA top-layer were deposited onto Ti6Al4V substrates, as shown in Figure 1. A Ti layer (about 30 μm) was first deposited as an initial bond coat (precoat) onto the substrates. After that, alternating deposition was performed using two torches that allowed for the use of independent processing parameters and divided into three steps. For example, the plasma power, flow rate of plasma gas (Ar/H_2), and powder feeding rate (Ti/HA) were changed from the parameters for Ti of 27.5 kW, 60/3 L min^{-1}, and 20/0 g min^{-1}, respectively, to 29.8 kW, 56/5 L min^{-1}, and 15/5 g min^{-1} so that Ti gradually decreased and HA simultaneously increased during deposition. Accordingly, the next step was to increase input power levels and to decrease the feeding rate ratio of Ti and HA powders, in addition to change the flow rate of plasma gas mixtures (Ar/H_2). Finally a 30 μm thick HA top-layer was plasma-sprayed onto the alternating layer. The plasma spray parameters for graded coatings were listed in Table I. Monolithic HA coating was also fabricated for comparison using the parameters for HA top-layer. Coating thickness for the two specimens was about 100 μm.

4.2. Heat treatment

In order to study the effect of heat treatment, the as-sprayed coatings were heat-treated at 400, 500, 600 and 700^{o}C for 1 h each at a heating rate of 5^{o}C/min in an air-circulated furnace. After treatment, the furnace was allowed to cool to room temperature. The optimal temperature was used for the coating loading drug or gafting RGD peptide.

4.3. Phase composition and morphology

Phases of the two types of the as-sprayed coatings were analyzed by an X-ray diffractometer (XRD, Shimadzu XD-D1, Kyoto, Japan) operated at 30 kV and 30 mA. A Fourier transform infrared (FTIR) spectroscopy (Bomem DA8.3, Hartman & Braun, Canada) in reflection absorption mode with a spectral resolution of 1 cm^{-1}, was used to characterize the various functional groups on the coating surface. The microstructure/microchemistry was characterized under field emission scanning electron microscope (FESEM) (Hitachi S-4200, Hitachi, Tokyo, Japan) equipped with an energy dispersive spectrometer (EDS, Noran Instrument Inc., Middleton, WI, USA). The Ca, P, and Ti concentration profiles of the graded coatings were measured using point analysis of EDS. Specimens for cross-sectional microscopy were prepared by mounting the coated specimens in epoxy resin, followed by polishing through 1 μm alumina.

4.4. Bond strength measurement

The plasma sprayed coating for load-bearing applications must be evaluated by fatigue ability due to the cyclic nature of in vivo loading. For the investigation of the fatigue resistance, the coated samples were fatigued under cyclic three-point bending test in air at room temperature using Shimadzu servopulser 48000 system (Kyoto, Japan). The fatigued samples were 50 mm in length, 10 mm in width, 3 mm in thickness with a gauge length of 40 mm. A cyclic loading of 280 MPa, which corresponds with the reported maximum bending stress of a clinically implant subjected to in vitro circumstances, with a stress ratio of S_{min}/S_{max} = zero was imposed at 5 Hz up to 1 million cycles, and then performing tensile bond strength and corrosion tests. Bond strength (or adhesive strength) of the two coatings before and after cyclic fatigue was used to represent the present pull-out test results using an EZ-Test machine (Shimadzu, Kyoto, Japan) at a loading rate of 0.5 mm/min. In doing the testing, a 2.7 mm dia. aluminum pull stud (Quad Group, Spokane, WA) was bonded to the coated surface with a solid epoxy and then cured at 150^{o}C for 1 h in oven.[3] After the coated specimen/stud assembly was gripped on a platen, the stud was then pulled down against the platen until failure. The maximum fracture force can be recorded and averaged to obtain the mean value and standard derivation. The number of measurements is twelve for each group.

4.5. Electrochemical testing

After fatigue and heat treatment, the coatings were electrochemically measured, in addition to as-sprayed coatings. The electrochemical measurements carried out on the samples included open circuit potential (OCP)-time measurements and potentiodynamic polarization in Hank's Balanced Salt Solution (HBSS), using a CHI 660A electrochemical system (CH Instrument, Austin, Texas). For OCP measurement, only two electrodes (working electrode and reference electrode) were involved, while for potentiodynamic polarization method a conventional three-electrode cell was used. A saturated calomel reference electrode (SCE) and a platinum counter electrode were employed. The sample surface was cleaned by distilled water. Deaerated conditions under N_2 gas purging and a temperature of 37°C were used for in vitro experiments. The evaluation of potentiodynamic polarization was started after immersion

in HBSS for 1 h. The scanned potential range varied from -1 V up to 2 V toward the anodic direction at a sweep rate of 0.5 mV/s in the Tafel mode. Six measurements were performed for each group. Corrosion potential and corrosion current were provided after being analyzed by the software.

4.6. In vitro release profile

Gentamicin is chosen as the drug model for its broad spectrum, effectiveness in treating osteomyelitis, and capacity for preventing osseous *staphylococcal* infections. Before loading the drug into the implant, the used drug was dissolved into pH 7.0 Gibco Dulbecco's phosphate-buffered saline (Invitrogen, Carlsbad, CA) without calcium and magnesium ions. Then, each sample was coated separately with 3 mL of drug solution, continually removed, and replaced into fresh immersion solution at regular intervals. The amount of gentamicin released was determined at 332 nm using a UV/VIS spectrophotometer (V-630, JASCO, Tokyo, Japan). For each antibiotics/implant combination, at least three parallel experiments were tested. In addition, SEM was also used to characterize the coated samples before and after release studies.

4.7. Evaluation of RGD grafting

Before RGDC grafting, all specimens were ultrasonically cleaned with dry ethanol for 10 min and dried at 60℃. Then, metal samples were sterilized via autoclave at 120^{o}C for 30 min). For RGDC immobilization, 100 μl of 1 mM RGDC solution in water was spin-coated onto the coating surfaces and air dried. MG63 human osteoblast-like cells were suspended in Dulbecco's modified Eagle's medium (DMEM, Gibco, Langley, OK) supplemented with 10% fetal bovine serum (Gibco, Langley, OK) and antibiotics (1% of a penicillin (10,000 U/ml)/streptomycin (10,000 mg/ml) solution (Gibco, Langley, OK). The cells were plated at a density of 2×10^4 cells/mL in 24-well plates containing various steriled samples. Plates were cultured in standard conditions at 37^{o}C and 95% humidity, and 5% CO_2.

The quantification of the adhered cells was performed by measuring their mitochondrial dehydrogenase activity using MTT assay. After 1, 4 and 24 h, the cells were treated with 5 mg/mL of thiazolyl blue tetrazolium bromide (Sigma, St. Louis, MO) in PBS (Gibco, Langley, OK) and incubated in the humidified atmosphere of 5% CO_2. After culture for 4 h, dimethyl sulfoxide (J.T. Baker, Phillipsburg, NJ) was used and the optical density was measured at the absorbance of 550 nm. The morphology of the cells adhering on coating surface was observed by SEM.

4.8. Statistical analysis

One-way analysis of variance (ANOVA) was used to evaluate the significant differences between the means in bond strength and electrochemical data. Scheffe's multiple comparison test was used to determine the significance of the standard deviations in the data of the various coated samples. In all cases, the results were considered statistically different at $p < 0.05$.

5. 結果與討論

5.1. Characterization of as-spayed coatings

In Fig. 1 the plasma-sprayed coatings generally have lower apatite crystallinity than HA powders used for plasma spray. Besides the broadening of apatite peaks and increased intensity of CaO phase, TCP phases were observed in monolithic HA and graded coatings. The high temperature involved in plasma spray process had obviously enhanced the decomposition of apatite as well as chemical reactions within HA phase. Since its top-layer

comprised HA phase of roughly 30 μm, it is reasonable that surface phase composition of the graded coatings detected by XRD was almost same as that of monolithic HA coatings. Similarly, both monolithic HA coating and graded coating should consistently exhibit many absorption bands of apatite structure in its FTIR reflection spectrum (Fig. 2). The broad band at 980-1120 cm^{-1} in FTIR reflection spectra of the two coatings, probably resulted from overlapping apatite and TCP signals, were attributed to HPO_4/PO_4 functional groups. The bands between 600 and 560 cm^{-1} were suggested to result from the vibrational mode of PO_4 groups. In contrast to those of HA powder, the decrease of the stretching mode at 3570 cm^{-1} and the librational mode at 630 cm^{-1} of OH groups, suggested the OH release of a hydroxylated HA structure that occurred in the two coatings. Additionally, the split sharp bands at 570, 600, 1050, and 1110 cm^{-1} indicated a well-crystallized apatite powder used for plasma spray.

Despite their different deposition processing, the two coatings had a similar morphology that had patches of smooth and shiny glassy films and irregularly-shaped particles (Fig. 3 (a)). Randomly distributed pores of different sizes and microcracks were also observed. The surface morphology depended strongly on the sizes and shapes of the feeding powder particles. During plasma spraying, small size powder was completely melted and formed a glassy phase during fast cooling, while larger size powder, such as the one used in the present study, was only partially melted resulting in a coating morphology comprising the observed irregularly-shaped particles. This observation is consistent with the earlier-discussed XRD results (e.g. broadening in apatite peaks).

The cross-sectional SEM micrographs showed that the layer defects between the splats within coatings are observed to run roughly parallel to the coating surface, as shown in Fig. 3 (b). Besides, there were a lot of perpendicular defects inside the coatings, e.g., pores and cracks. These plasma spray-induced layer defects were frequently observed in plasma sprayed HA and other coatings. It was found that the microstructure of graded coatings gradually transferred from Ti bond coat to HA topcoat accompanied with the change in composition distribution through coating thickness.

Chemical distribution of three major elements, Ca, P and Ti, in the graded coatings cross-section was studied using SEM-EDS technique, as also shown in Figure 3 (c). In doing through-thickness chemical analysis of the coatings, a series of point analyses were made on the polished cross section of the coating. These elemental point analysis illustrated the graded coatings were with a controlled compositional gradient. The alternating layer within the coating had a gradually decreasing concentration of the Ti toward the outer surface with the exception of initial bond coat, along with a gradually increasing Ca and P contents up to a bioactive top-layer composed of an apatite. The composition changes were so gradual that the interface between the substrate and the coating layer as well as the boundaries among the phases within the coating layer should seem to be tightly bonded, which was the main purpose to be achieved. The measured Ca/P ratio on HA top layer was in the range of 1.9-2.1, higher than the stoichiometric Ca/P ratio (1.67) of HA, and also observed in other plasma-sprayed HA coatings due to the fact that a large quantity of phosphorus was vaporized during the high temperature plasma spray process.

5.2. Characterization of fatigued coatings

The graded HA/Ti composite coatings had a significantly ($p < 0.05$) greater bond strength of 23.1 ± 3.4 MPa compared to that of monolithic HA coatings (14.2 ± 3.1 MPa). It is believed to be attributable to the Ti affinity and gradient coating processes [9,10]. The existence of an intermixed layer resulted in the achievement of a good adhesion of the deposited coating to the substrate. As is known, the cracks and weakness at HA-Ti interfaces

probably result from mismatch between the coefficients of thermal expansion (CTEs) of these materials. The formation of an intermixed layer in the functionally graded coating may resist the external stress produced by the unmatched CTEs. Hence the graded coatings structure may produce stronger mechanical interlocking, as suggested by Inagaki et al. [10] The major feature of the present paper resided in the facts that the Ti component in the intermixed zone with relatively good affinity to the Ti6Al4V substrate was sandwiched between the metallic substrate and the top biocoating, so that even when the HA surface layer of the composite coating was absorbed in the bone tissue, direct contact between the metallic substrate and the bone tissue can be prevented. Post-test observations indicated that the failure of monolithic HA coatings mostly occurred at the HA-Ti interface. The graded coatings mainly fractured in the HA-rich layer.

All joints in the human body are constantly subjected to fatigue loading during the simple actions of everyday living. A particular weakness in the mechanical properties of bioceramic coatings resides in their fatigue resistance. After cyclic fatigue in air for 1 million cycles, the average strength of monolithic HA coatings bonded to substrate significantly ($p < 0.05$) declined from 14.2 MPa, the as-sprayed strength, down to 10.9 MPa. The stability of monolithic HA coating was apparently affected by the cyclic loading, with a remarkable decrease of 23%. The fatigue-induced degradation in bond strength could arise from a poor bonding between ceramic coating and metal substrate associated with adhesive failure. The graded coatings did not change significantly ($p > 0.05$) over the 1 million-cycle test, keeping the bond strength around 22 MPa. The graded coatings appeared more stable than monolithic HA coatings as fatigued in air at room temperature.

The open circuit potential over time of the two coatings in HBSS before and after cyclic fatigue is depicted in Fig. 4. The OCP of both as-sprayed samples shifted towards active direction after immersion due to the dissolution that occurred at the coating surface, followed by reaching a steady state. Compared to as-sprayed, the two fatigued samples showed a lower initial potential and attained more negative potential values, indicating an inferior corrosion behavior. In contrast to monolithic HA coatings, when subjected to cyclic fatigue, the graded coatings might exhibit a better corrosion resistance during the OCP measurements.

Fig. 5 shows the typical potentiodynamic polarization curves of the plasma-sprayed coatings without and with fatigue. As corrosion potential was concerned, no significant differences ($p > 0.05$) were observed between the two as-sprayed coatings. In addition, the corrosion current density of the graded coatings was close to that of monolithic HA coatings because the occurrence of corrosion was the same on the surface for both coatings made of HA top-layer. These results agreed with the OCP curves.

After cyclic fatigue, corrosion potential (-505 ± 69 mV vs. SCE) of the monolithic HA coating decreased significantly ($p < 0.05$) to the value of -875 ± 78 mV. The HA coatings before and after fatigue had a current density of 91 ± 25 and 480 ± 125 nA/cm^2, respectively, revealing the significant difference ($p < 0.05$). The results confirmed that fatigued HA coatings exhibited a worse electrochemical behavior than corresponding as-sprayed coatings by virtue of more active corrosion potential and greater current, although both curves were characterized by a very similar trend. It is worthwhile to note that monolithic HA coatings with fatigue indicated an obvious breakdown potential of around 0.8 V as compared to the other coatings, possibly due to fatigue-induced delaminated structure that led to the penetration of solution into the coating/substrate interface through the perpendicular and/or parallel defects. The comparative study of the corrosion behavior of the graded specimens elicited that the coatings after fatigue presented a more negative corrosion potential value of -720 ± 99 mV than -576 ± 87 mV obtained from the coatings without fatigue, but did not significantly differ ($p > 0.05$). The results suggested that graded coatings might be not

apparently susceptible to influence of cyclic fatigue in air for 1 million cycles possibly due to the good cohesion degree of the coating, in accordance with the results from bond strength evaluation. As for current density, it could be found that the average values of the graded coatings of between 142 and 210 nA/cm^2 were independent on fatigue. To this end, the fatigue could promote HA coatings to be unstable.

5.3. Characterization of heat-treated coatings

Compared to the as-sprayed coating, heat-treated coatings had higher apatite crystallinity and a smaller amount of TCP and CaO phases (Fig. 6). The 400°C temperature did not affect the phase evolution. When the treatment temperature was raised to 500°C, the peaks became sharper. Using the integrated area of (211), (112) and (300) peaks of apatite phase, the crystallinity of heat-treated coatings was about three-fold greater than that of the as-sprayed coating, and slightly increased with an increase in treatment temperature.

Similarly, after post-deposition treatment in air at 500–700°C with the exception of 400°C, the sharper PO_4 stretching mode at 604 and 573 cm^{-1} and the two more appreciable adsorption bands at 970–1130 cm^{-1} demonstrated an increased crystallinity. The appearance of the absorption band at 630 cm^{-1} of the OH group suggested the reestablishment of a hydroxylated HA structure. Atmospheric moisture can react with amorphous oxyapatite so that OH groups are recovered promoting the reconstitution of amorphous oxyapatite into crystalline oxyhydroxyapatite. In addition to enhancing coating crystallinity, the presently used heat treatment could effectively convert non-apatite phases such as TCP into apatite, in agreement with previous studies [14,17]. Although higher-temperature treatment can help hasten the amorphous-crystalline phase transformation, it was practical to use lower heat-treatment temperatures to avoid serious irreversible structural and property changes to the Ti alloy substrate, as well as Ti particles within the graded coatings.

The cross-sectional pictures of 400°C-treatment coatings, similar to the as-sprayed coating, showed that the layer defects between the splats within coatings, as indicated by arrows, were observed to run roughly parallel to the coating surface. Additionally, there were a lot of perpendicular defects inside the coatings, e.g., pores and cracks. These plasma spray-induced layer defects were frequently observed in plasma sprayed HA and other coatings, which were determined to be amorphous with micro-Raman spectroscopy and nano-indentation techniques [24]. After post-deposition heat treatment at 500–700°C, layer defects appearing within plasma-sprayed coatings were deceased. The differences in the CTE (coefficient of thermal expansion) caused by the annealing might more or less contribute to microstructure changes because different phases possess different CTEs (HA: $11.5 \times 10^{-6}{}^{o}C^{-1}$, TCP: $14.2 \times 10^{-6}{}^{o}C^{-1}$, Ti: $8.5 \times 10^{-6}{}^{o}C^{-1}$) [25, 26]. In addition, this can be explained in terms of the heat treatment during which the atoms gained high kinetic energy and diffused much faster than at room temperature [16]. The faster diffusion of the atoms speeded up the phase transition and affected the coating appearance.

The bond strength of the as-sprayed coatings was 23.1 ± 3.4 MPa. After heat treatment at 400, 500, 600 and 700°C, the value became 21.1, 22.0, 25.6 and 14.1 MPa, respectively, indicating there was significantly different ($p < 0.05$). Clearly, the bond strengths of the specimens heat treated at 400–600°C were not significantly higher than that of the as-sprayed coating ($p > 0.05$). Statistical analysis using Scheffe's multiple comparison test showed that the bond strength of 700°C-treatment coatings significantly declined by about 39%. The 600°C-treatment coating had greater bond strength than the as-sprayed coating, although there was not significantly different ($p > 0.05$). The differences in bond strength can be explained in terms of stress relief and microstructural changes. When heat-treated at higher temperatures such as 700°C, the regions near the substrate may result in a larger amount of cracks caused by the large volume shrinkage during crystallization and phase transformation. In turn, it is detrimental to the bonding strength of the coating, although it possesses a higher

degree of crystallinity.

The OCP-time plots of the coating samples heat-treated at different temperatures as a function of time along with the as-sprayed coating are shown in Fig. 7. It seems that the as-sprayed coating was in a steady state possibly due to the apatite precipitation, although with a more negative initial potential of -0.47 V. On the contrary, all heat-treated samples except the coating heat-treated at 400°C showed a higher initial OCP, tending to a decreased potential ranging from -0.10 V to -0.25 V after OCP scanning for 5 h. Fig. 7 also shows the typical potentiodynamic polarization curves of the plasma-sprayed coatings without and with heat treatment in deaerated HBSS at 37°C. All electrochemical parameters, including corrosion potential (E_{corr}), current density (i_{corr}), and polarization resistance (R_p), of coating samples are also compiled in Table 1. Concerning the corrosion potential, there are significant differences ($p < 0.05$) among all test samples. After heat treatment at 400, 500, 600 and 700°C, corrosion potentials of the heat-treated samples were found to be -598, -518, -464 and -692 mV (vs. SCE), respectively. Our results confirmed that the 600°C-treatment coating exhibited a significantly better corrosion-resistance than all the other coatings by virtue of a more noble corrosion potential, although all polarization curves were characterized by a very similar trend.

The corrosion current density and polarization resistance of the samples were determined from the potentiodynamic polarization curves using the Tafel extrapolation method. As for the current density, it was determined that the average values of the heat-treated coatings of between 83 and 153 nA/cm^2, which were comparable to that of the as-sprayed coating (142 nA/cm^2), were dependent on treatment temperature, revealing the significant difference ($p < 0.05$). It is worthwhile to note that heat-treated coatings at 700°C indicated a lower corrosion potential and larger corrosion current density as compared to the 500°C- and 600°C-treated coatings, possibly due to higher temperature-induced structure changes that led to the penetration of solution into the coating/substrate interface through perpendicular and/or parallel defects. In contrast to the current density, there was an increase in the R_p values by about a factor of two, illustrating that heat treatment endowed the coatings better corrosion resistance except for the treatment at 400°C.

The critical factors influencing the corrosion behavior of HA-based coatings are the quality (crystallinity, purity, residual stress and ion substitution in the apatite lattice) and structure (porosity and cracks) [27]. The porosity is a characteristic of plasma sprayed coatings and strongly affects their corrosion-resistance. Generally speaking, the corrosion rate increases with increasing porosity of the coatings. The electrolyte infiltrates into the inner portion of the coating through structural imperfections such as pores and cracks or pinholes existing in the coating, and it comes into contact with the deeper portion of the coating [27], causing corrosion. The obtained polarization resistance (R_p) can be used to determine the porosity that corresponds simply to the ratio of the polarization resistance of the uncoated substrates and the coated samples [28]. Using a modified equation, the ratio of $P_s/P_{hs} = R_{p,hs}/R_{p,s}$ can be used to represent the change in porosity, where P_s and P_{hs} are the porosity of the as-sprayed and heat-treated coatings, and $R_{p,s}$ and $R_{p,hs}$ are the polarization resistance of the as-sprayed and heat-treated coatings, respectively. Substituting the obtained R_p values into the above-mentioned equation, it is obvious that P_s/P_{hs} is approximately two for the samples heat-treated at temperature greater than 400°C, indicating that there was a positive effect on the reduction of the porosity occurred in those samples. This was because the heat treatment apparently reduced plasma spray-induced layer defects, as described earlier in the morphology change, resulting in heat-treated coatings possessing higher corrosion-resistance. More importantly, the *in vitro* electrochemical test results indicated that treatment at 600°C had a more beneficial and desired effect on corrosion behavior than the as-sprayed and the other three heat-treated samples at 400, 500 and 700°C from the viewpoints of R_p and corrosion potential.

5.4. In vitro drug release

Gentamicin loading onto coatings is a clinically relevant concept in the context of total joint arthroplasty and dental surgery. We used antibiotic-soaked coatings in an *in vitro* drug release study. The appearances of the heat-treated coating surfaces were similar to those of as-sprayed coatings, which had well-flattened splats and shiny glassy films and irregularly shaped particles, as shown in Fig. 8a. Randomly distributed pores of different sizes as well as microcracks were also observed. Gentamicin might incorporate into the pore within the plasma sprayed coating. In contrast to the image in Fig. 3a, the gentamicin-loaded surface became much smoother and quite uniform, but fractures were visible possibly due to drying (Fig. 8b). After drug release, coating morphologies are similar to those without drug loading (Figs. 8c, d).

Gentamicin release profiles from the two coatings in PBS as a function of time are shown in Fig. 9. Generally, the release curves can be separated into an initial fast release, followed by a slow release pattern. The fast release is mainly caused by the dissolution of the drug that is physically adsorbed on coating implants, and the slow release may be attributed to chemically adsorbed drugs. It can be seen that during the fast release, the rate of the untreated coatings was larger than that of the heat-treated coatings. It is noted that, at the initial 1 h, the two coatings released almost entirely gentamicin. Osteoconductive coatings have the potential to serve as drug carriers to prevent infection in the setting of total joint arthroplasty and dental therapy [29].

5.5. RGD grafting

An ideal biomaterial for bone repair and replacement would administer the appropriate signals to direct the processes of osteogenesis, such as cell attachment, proliferation, differentiation, matrix deposition and ultimately mineralization of extracellular matrix. As aforementioned, RGD peptide can induce cell attachment. The MTT assay indicated there are no significant differences between all samples with or without RGDC peptide. The effect of heat treatment on cell attachments also elucidated similar results. The morphology of attached cells remained rounded morphology and had no differences among all samples after incubation for 1 day. Interestingly, cells were better spread on heat-treated coatings without RGDC grafting surface after 4 h incubation. It seems the presence of extracellular matrix secretion. The morphology of cells attached to the samples surface would not be affected by RGDC physical immobilization. This might be attributed to the degradation of physically adhered RGDC on samples surface after contacting with culture medium [30]. Two important design factors, when using RGD, are addressed: (1) the spatial distribution or concentration of peptides incorporated into biomimetic materials and (2) the spacer for peptide modification, which enables peptide sequences to freely extend outward of the Network [21]. Sawyer et al. suggested a potential therapeutic benefit for functionalizing HA with RGD, however such a benefit will likely depend upon the RGD density [23]. Hern et al. showed that cells adhered to the RGD modified surface with a PEG spacer (MW 3400) at low surface density (0.01 pmol/cm^2), although the surface modified with RGD without the spacer exhibited limited cell adhesion even at a higher surface density (1 pmol/cm^2) [31]. To clarify the role of RGD peptide on bone tissue, a further investigation is needed.

6. 結　論

The results of the comparative study indicated that functionally graded HA/Ti composite coatings had better mechanical properties than monolithic HA coatings through bond strength evaluation, although the two types of as-sprayed coatings possessed the same surface chemistry and morphology. It is no doubt that the properties of monolithic HA coatings were susceptible to be declined when subjected to fatigue. However, the graded coatings were able

to survive 10 million cycles of loading of 280 MPa in air without significantly reduced bond strength. In addition, the graded coatings seemed to possess a better corrosion-resistant ability. The presently used functionally graded coating method for the preparation of HA/Ti implant may play a predominant role in enhancing the characteristics of plasma-sprayed coatings.

In the second year, after heat treatment at 500–700^{o}C, the graded coatings had an enhanced crystallinity by a factor of three but a temperature-sensitive bond strength. Among the treatment temperatures, 600^{o}C seems to endow the graded coating with better corrosion-resistance with an increased polarization resistance value by approximately two times as compared to the as-sprayed samples. Improved corrosion resistance was due to a coating surface modification with higher degree of crystallinity and less dissoluble non-apatite phases (TCP), as well as a reduction in coating defects when plasma-sprayed coatings were subjected to post-deposition heat treatment. Gentamicin loading might provide effective release at early time points (up to 1 h). The MTT assay indicated there are no significant differences between all samples with or without RGDC peptide.

7. 成果自評

The first-year study of this two-year project featured the investigation of processing and properties of graded HA/Ti coatings. The results have been published in Journal of Biomedical Materials Research Part B 2006;78B:146-152. In the second year, we evaluated the effect of heat treatment on characterization of graded coatings. In addition, drug-delivery and RGD peptide grafting following heat treatment were also examined. The interesting results of the heat-treated coatings loaded gentamicin have been reported in 1st ABMC [28] as invited lecture and collected in a book entitled “Biomaterials in Asia” [32]. As for the RGD grafting, the application of patent is being evaluated.

8. 參考文獻

1. de GootK, Geesink R, Klein CPAT, Serekian P. Plasma sprayed coatings of hydroxylapatite. J Biomed Mater Res 1987;21:1375–1381.
2. Friedman RJ, Black J, Galante JO, Jacobs JJ, Skinner HB. Current concepts in orthopaedic biomaterials and implant fixation. J Bone Joint Surg 1993;75A:1086-1109.
3. Ding SJ, Ju CP, Chern Lin JH. Immersion behavior of RF magnetron-assisted sputtered hydroxyapatite/titanium coatings in simulated body fluid. J Biomed Mater Res 1999;47:551–563.
4. Filiaggi MJ, Pilliar RM, Abdulla D. Evaluating sol-gel ceramic thin films for metal implant applications. II. Adhesion and fatigue properties of zirconia films on Ti-6AI-4V. J Biomed Mater Res 1996;33:239–256.
5. Cook SD, Thomas KA, Kay JF. Experimental coating defects in hydroxyapatite-coated implants. Clin Orthop 1991;265:280-290.
6. Gu YW, Khor KA, Pan D, Cheang P. Activity of plasma sprayed yttria stabilized zirconia reinforced hydroxyapatite/Ti-6Al-4V composite coatings in simulated body fluid. Biomaterials 2004;25:3177–3185.
7. Kangasniemi IM, Verheyen CC, van der Velde EA, de Groot K. In vivo tensile testing of fluorapatite and hydroxylapatite plasma-sprayed coatings. J Biomed Mater Res 1994;28:563–572.
8. Fathi MH, Salehi M, Saatchi A, Mortazavi V, Moosavi SB. Novel double layer hydroxyapatite (HA)/Ti coating for biocompatibility improvement of metallic implants. Surf Eng 2001;17:459–464.
9. Gruner H. Coating of implants. Chem Abstr 1987;106:55966g.
10. Inagaki M, Yokogawa Y, Kameyama T. Apatite/titanium composite coatings on titanium

or titanium alloy by RF plasma-spraying process. Thin Solid Films 2001;386:222–226.
11. Lu YP, Li MS, Li ST, Wang ZG, Zhu RF. Plasma-sprayed hydroxyapatite+titania composite bond coat for hydroxyapatite coating on titanium substrate. Biomaterials 2004;25:4393–4403.
12. Chou L, Marek B, Wagner WR. Effects of hydroxylapatite coating crystallinity on biosolubility, cell attachment efficiency and proliferation in vitro. Biomaterials 1999;20:977–985.
13. Maxian SH, Zawadsky JP, Dunn MG. Mechanical and histological evaluation of amorphous calcium phosphate and poorly crystallized hydroxyapatite coatings on titanium implants. J Biomed Mater Res 1993;27:717–728.
14. Ding SJ, Huang TH, Kao CT. Immersion behavior of plasma-sprayed modified hydroxyapatite coatings after heat treatment. Surf Coat Tech 2003;165:248–257.
15. Weng J, Cal T, Chen J, Zhang X. Significance of water promoting amorphous to crystalline conversion of apatite in plasma sprayed coatings. J Mater Sci Lett 1995;14:211–213.
16. Chen J, Tong W, Cao Y, Feng J, Zhang X. Effect of atmosphere on phase transformation in plasma-sprayed hydroxyapatite coatings during heat treatment. J Biomed Mater Res 1997;34:15–20.
17. Chen CC, Ding SJ. Effect of heat treatment on characteristics of plasma sprayed hydroxyapatite coatings. Mater Transact 2006;47:935–940.
18. Akashi A, Matsuya Y, Unemori M, Akamine A. Release profile of antimicrobial agents from α-tricalcium phosphate cement. Biomaterials 2001;22:2713–2717.
19. Schofield SC, Berno B, Langman M, Hall G, Filiaggi MJ. Gelled calcium polyphosphate matrices delay antibiotic release. J Dent Res 2006;85:643–647.
20. Sawyer AA, Weeks DM, Kelpke SS, McCracken MS, Bellis SL. The effect of the addition of a polyglutamate motif to RGD on peptide tethering to hydroxyapatite and the promotion of mesenchymal stem cell adhesion. Biomaterials 2005;26:7046–7056.
21. Shin H, Jo S, Mikos AG. Biomimetic materials for tissue engineering. Biomaterials 2003;24:4353–4364.
22. Porte-Durrieu MC, Guillemot F, Pallu S, Labrugere C, Brouillaud B, Bareille R, Amedee J, Barthe N, Dard M, Baquey C. Cyclo-(DfKRG) peptide grafting onto Ti–6Al–4V: physical characterization andinterest towards human osteoprogenitor cells adhesion. Biomaterials 2004;25:4837–4846.
23. Sawyer AA, Hennessy KM, Bellis SL. Regulation of mesenchymal stem cell attachment and spreading on hydroxyapatite by RGD peptides and adsorbed serum proteins Biomaterials 2005;26:1467–1475.
24. Wen J, Leng Y, Chen J, Zhang C. Chemical gradient in plasma-sprayed HA coatings. Biomaterials 2000;21:1339–1343.
25. Sergo V, Sbaizero O, Clarke DR. Mechanical and chemical consequences of the residual sresses in plasma sprayed hydroxyapatite coatings. Biomaterials 1997;18:477–482.
26. Milosevski M, Bossert J, Milosevski D, Gruevska N. Preparation and properties of dense and porous calcium phosphate. Ceram Int 1999;25:693–696.
27. Cao Y, Weng J, Chen J, Feng J, Yang Z, Zhang X. Water vapour-treated hydroxyapatite coatings after plasma spraying and their characteristics. Biomaterials 1996;17:419–424.
28. Ding SJ, Chien PJ, Ho CC. Gradient hydroxyapatite/titanium coating implants. The First Asian Biomaterials Congress (1st ABMC), Tsukuba, Japan, Dec 6-8, 2007, accepted.
29. Radin S, Campbellt JT, Ducheyne P, Cuckler JM. Calcium phosphate ceramic coatings as carriers of vancomvcin. Biomaterials 1997;18:777–782.
30. Connelly JT, García AJ, Levenston ME. Inhibition of in vitro chondrogenesis in RGD-modified three-dimensional alginate gels. Biomaterials 2007;28:1071–1083.
31. Hern DL, Hubbell JA. Incorporation of adhesion peptides into nonadhesive hydrogels useful for tissue resurfacing. J Biomed Mater Res 1998;39:266–76.
32. Ding SJ, Chen CC, Ho CC. Biostable gradient coating implants with drug release. in "Biomaterials in Asia", Tetsuya Tateishi, Eds., World Scientific Publishing, Kerala, 2008,

pp.. (Invited paper).

Table 1 Mean and standard derivation values of electrochemical parameters of the as-sprayed coating and heat-treated graded coatings at different temperatures after electrochemical test

Coating		E_{corr} (mV)	i_{corr} (nA·cm^{-2})	R_p (kΩ·cm^2)
As-sprayed		-576 ± 87^{a,b,c}	142 ± 54^{a,b}	72 ± 16^{a}
Heat-treated (^{o}C)	400	-598 ± 60^{a,b}	134 ± 35^{a,b}	87 ± 29^{a}
	500	-518 ± 46^{b,c}	95 ± 25^{a,b}	162 ± 33^{b,c}
	600	-464 ± 58^{c}	83 ± 23^{a}	178 ± 49^{c}
	700	-692 ± 77^{a}	153 ± 39^{b}	103 ± 22^{a,b}

Number of samples is at least six in each subgroup.
Mean values followed by the same superscript letter in the same column are not significantly different ($p > 0.05$) according to Scheffe's *post-hoc* multiple comparisons.

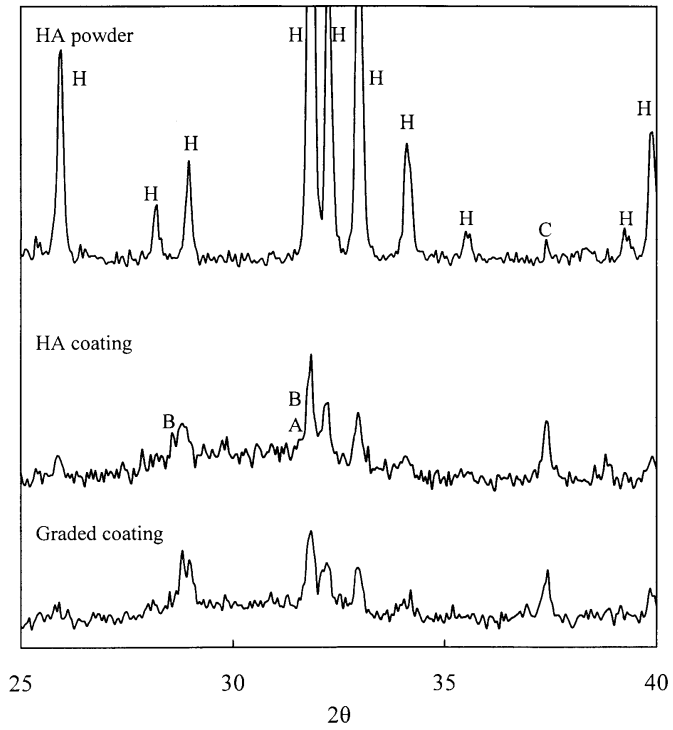

Figure 1. XRD patterns of the HA powder, monolithic HA coating, and graded coating (H: apatite; A: α-TCP; B: β-TCP; C: CaO).

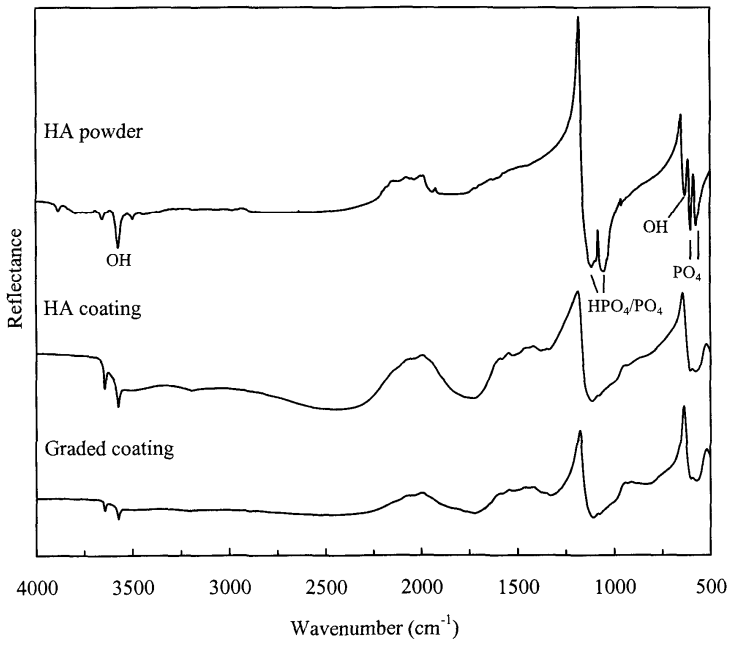

Figure 2. FTIR spectra of the HA powder, monolithic HA coating, and graded coating.

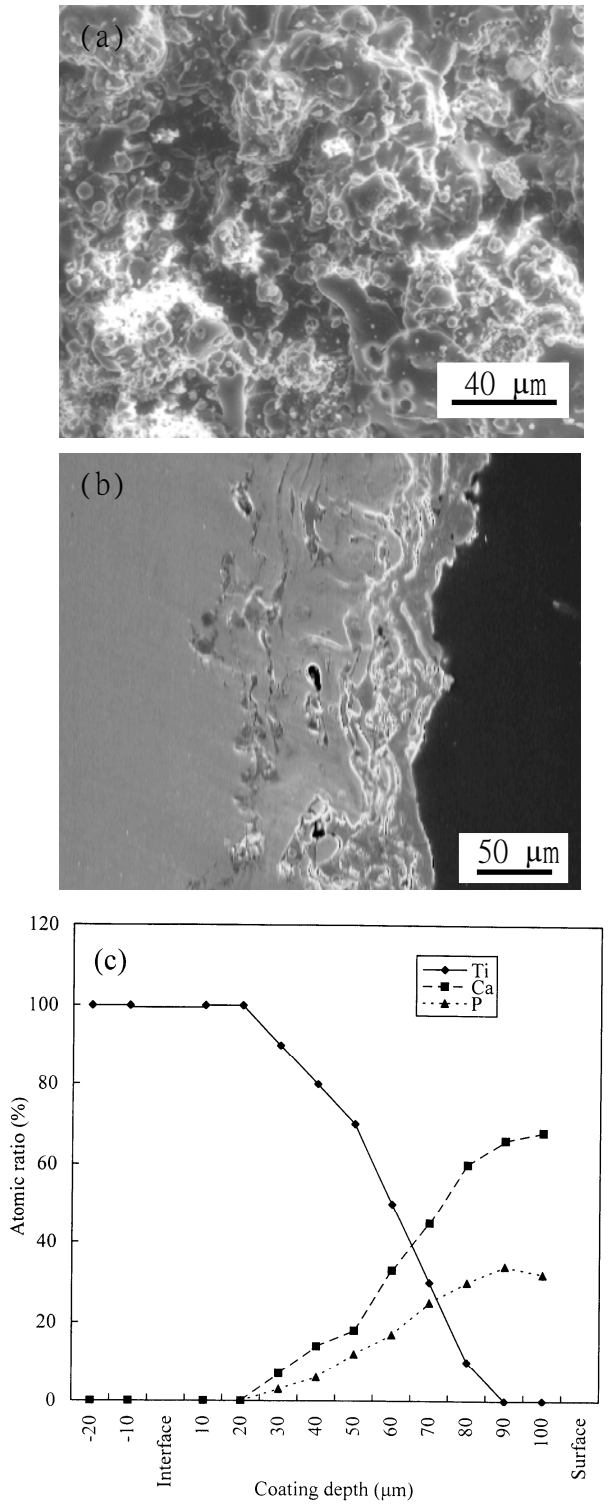

Figure 3. (a) Surface and (b) cross-sectional SEM micrographs and (c) elemental analyses of Ti, Ca and P through coating thickness of the graded coating.

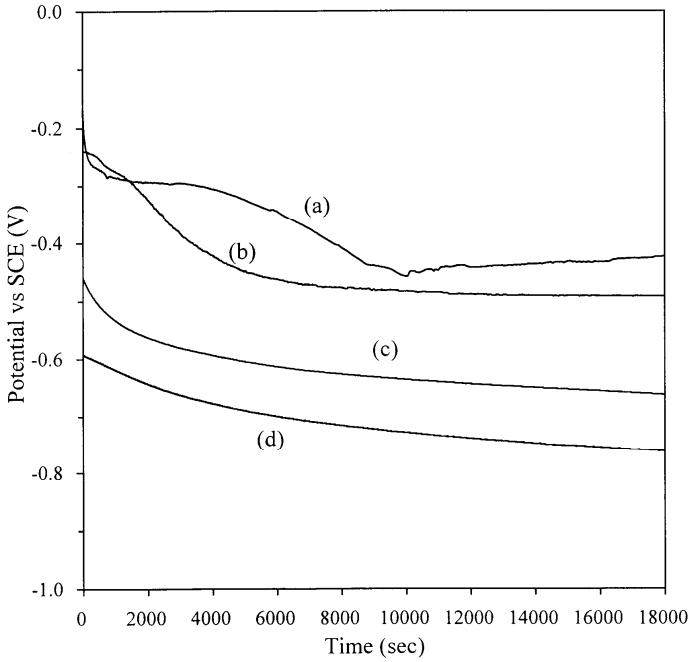

Figure 4. OCP of coated samples before and after cyclic fatigue. (a) HA coating without fatigue, (b) graded coating without fatigue, (c) graded coating with fatigue, and (d) HA coating with fatigue.

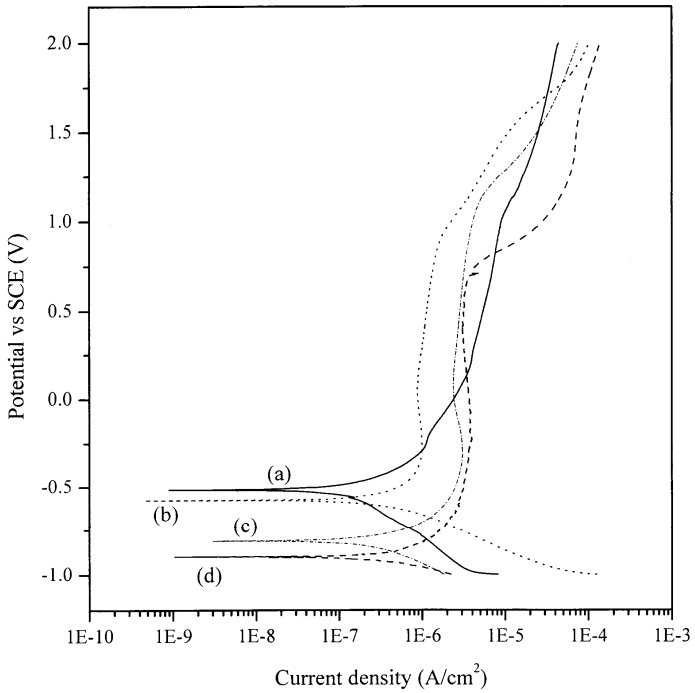

Figure 5. Typical polarization curves of coated samples before and after cyclic fatigue. (a) HA coating without fatigue, (b) graded coating without fatigue, (c) graded coating with fatigue, and (d) HA coating with fatigue.

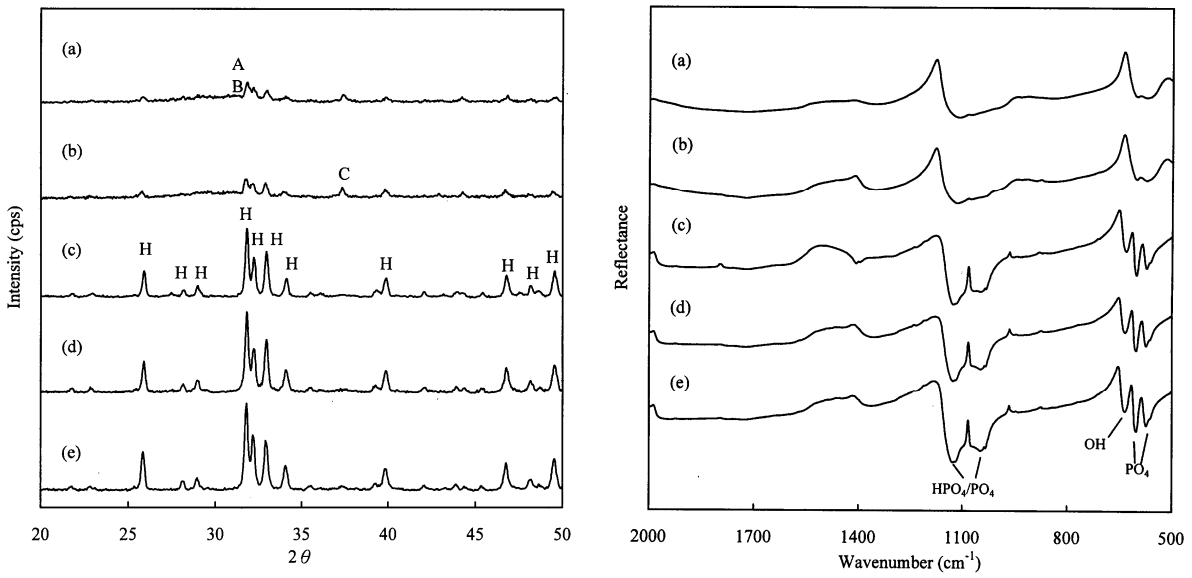

Figure 6. XRD patterns (left) and FTIR spectra (right) of the as-sprayed coating (a) and heat-treated coatings at 400°C (b), 500°C (c), 600°C (d), and 700°C (e). (H: apatite; A: α-TCP; B: β-TCP; C: CaO).

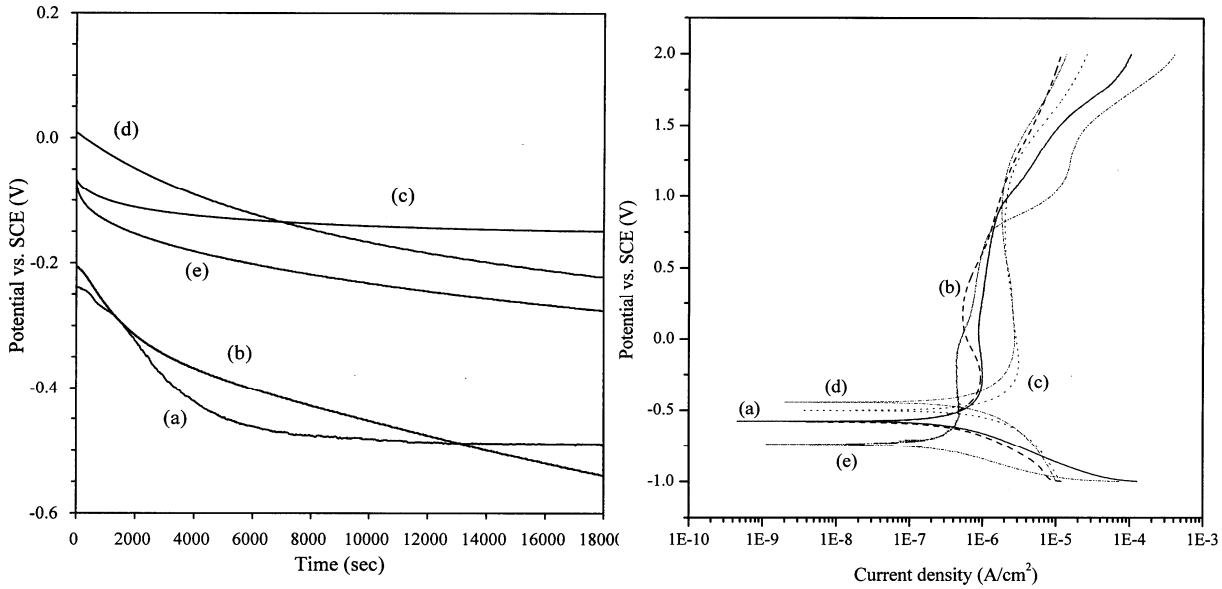

Figure 7. Open circuit potential-time (left) and typical polarization (right) curves of graded coatings before (a) and after heat treatment at 400°C (b), 500°C (c), 600°C (d), and 700°C (e) in deaerated HBSS at 37°C.

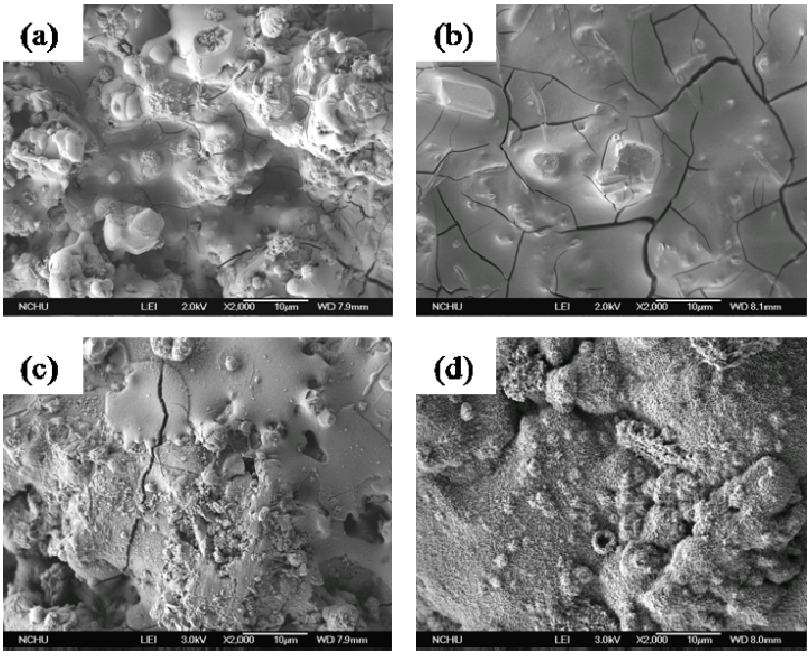

Figure 8. Scanning electron micrographs: as-sprayed coating (a) with gentamicin loading (b), the release of gentamicin for as-sprayed coating (c) and 600^{o}C-treatment coating (d).

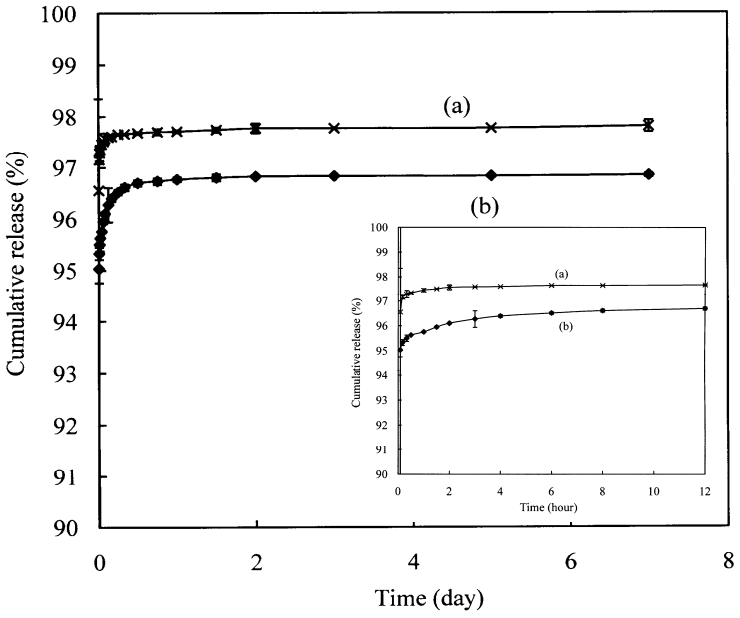

Figure 9. The release profiles of gentamicin as a function of time from coatings without (a) and with heat treatment at 600^{o}C (b). The insert is the short-term release profiles.

出席國際學術會議心得報告

計畫編號	NSC 95-2314-B-040-011-MY2
計畫名稱	含胜肽分子之氫氧基磷灰石/鈦功能性漸鍍層之特性研究
出國人員姓名 服務機關及職稱	丁信智 中山醫學大學　口腔材料科學所　教授
會議時間地點	96/9/9-96/9/14　加拿大 Banff
會議名稱	第 58 屆國際電化學年會
發表論文題目	Electrochemical behavior of heat-treated hydroxyapatite/titanium composite coatings

一、參加會議經過

本次第 58 屆國際電化學年會在加拿大班夫國家公園內的班夫中心國際會議廳舉行。會議發表分口頭及海報貼示，論文超過 1100 篇，會議期間每天早上 9 點有 1 小時的 plenary lecture，邀請電化學領域大師專題報告。整個會議研討涵蓋與電化學相關的各種不同議題，如生物電化學、感測器、鋰電池、材料腐蝕、生物燃料電池、電化學奈米科技、電催化等。並有電化學儀器設備商同時參展，會場討論氣氛十分熱絡。在 9/12 下午大會有半日遊的活動，本人自費參於 Lake Louise & Moraine Lake Tour，當晚並有晚宴。本人受第六屆亞洲電化學研討會主辦單位林修正教授所託，攜帶 demo 至會場。

二、與會心得

此研討會主要是由國際電化學學會主導，來自美加、歐洲及亞洲地區（大陸、日本及韓國）多位學者參與。台灣學者除我本人外，另有來自台灣科技大學化工系何國川教授實驗室博士生、成大醫工張憲彰教授、中興吳靖宙教授、大同張敏興教授等參加。電化學研究為一跨領域且理論、應用並重的學門，從與會中所發表的論文可知仍有相當大的研究空間。國際趨勢除能源主題外，似乎逐漸朝向運用電化學理論於分子級奈米科技。這次本人的論文發表，也與國外學者進行多次意見交流，並邀請數位國際友人參於台北第六屆亞洲電化學研討會。台灣電化學研究人才散佈在各領域如化工、材料、醫工、化學等，不過並沒有一個直接的電化學學會，但可喜的是經過數位教授努力，國際電化學學會支持，將在 2008，5/11-14 於台北舉辦第六屆亞洲電化學研討會。期待未來能舉辦更多國際型會議。

Electrochemical Behavior of Heat-Treated Hydroxyapatite/Titanium Composite Coatings

Shinn-Jyh Ding*, Po-Jen Chien
Institute of Oral Materials Science, Chung-Shan Medical University, Taichung 402, Taiwan
sjding@csmu.edu.tw

Hydroxyapatite (HA)-coated appliances plasma sprayed on the metallic substrates endow the orthopaedic and dental implants not only with bioactivity but also with a protective layer shielding the release of metal ions, in addition to bearing the loading. Nevertheless, the HA coating-metallic substrate bonding is still an unsolved problem for the long-term clinical use of the implant. To improve the coating-substrate bond strength and other properties, more recently, we developed functionally graded HA/Ti coatings consisting of an underlying Ti bond coat, the alternating layer, and an HA top-layer plasma-sprayed on titanium alloy substrates [1]. In this work, the major consideration was to examine the corrosion resistance of the potential graded coatings after various post-deposition heat treatments over 400-700^{o}C at 100^{o}C interval.

The results elicited that the heat treatment used led to recrystallization of amorphous calcium phosphate of as-sprayed coatings and gave rise to a higher crystallinity by a factor of 4-5 but temperature-sensitive bond strength. In contrast to the other three heat-treated coatings, the 500^{o}C-treated specimen had the maximum bond strength that was comparable to the as-sprayed coating of about 23 MPa. After post-deposition heat treatment, plasma spray-induced layer defects such as porosity within coatings were effectively reduced. As for the electrochemical results, although there was no significant difference in corrosion potential between as-sprayed coating and heat-treated coating at 500^{o}C, the current density of this heat-treated coating was significantly lower than that of the as-sprayed coating. Moreover, the heat-treated coating had a better corrosion-resistant ability with an increased polarization resistance value by approximately two times as compared to the as-sprayed specimen. Improved corrosion resistance was possibly due to a coating surface modification with higher crystallinity and less dissoluble non-apatite phases, as well as a reduction of coating defects [2] when the functionally graded coatings were subjected to post-deposition heat treatment.

On the basis of the data in this study, the heat treatment at 500^{o}C for 1 h in air, endowing with increased crystallinity and the reduced defects without significantly reduced bond strength, provided a better corrosion protection than the other three treatment temperatures.

Reference

[1] C.C. Chen, T.H. Huang, C.T. Kao, S.J. Ding, J. Biomed. Mater. Res. 78B (2006) 146.
[2] C.C. Chen, T.H. Huang, C.T. Kao, S.J. Ding, Electrochim. Acta 50 (2004) 1023.

Acknowledgement to National Science Council of the Republic of China (grant No. 95-2314-B-040-011-MY2).